FACULTÉ DES SCIENCES ET DE GÉNIE
Département de génie civil et génie des eaux

Cité universitaire
Québec, Canada G1V 0A6

model*EAU* Internship report

Internship of Maxime Roussel, monEAU project

AUTHOR/COAUTHORS	TEAM/GROUP
Maxime Roussel	model*EAU*

WRITTEN BY		LATEST REVISION BY	
Name	Maxime Roussel	**Name**	
Date	22/07/14	**Date**	

DOCUMENT FILE NAME	Internship report modelEAU
# PAGES	
REVISION NO.	

model*EAU*, Département de génie civil et génie des eaux
Université Laval
Pavillon Adrien-Pouliot - local 2974
1605 Avenue de la Médecine
Québec (qc) G1V 0A6, Canada

Téléphone: +1 (418) 656-5085
Télécopieur: +1 (418) 656-2928

peter.vanrolleghem@gci.ulaval.ca
http://modelEAU.fsg.ulaval.ca

INDEX

LIST OF FIGURES

LIST OF TABLES

ABSTRACT

In this report I summarize all the tasks that I carried out during my internship from May 19th until September 26th in model*EAU* research group, in the civil and water engineering department, University Laval.. During this period I was linked to the monEAU group led by Janlecy Castano Alferes. This internship was a very good opportunity to discover the research sector and the culture in Québec and more generally in Canada. During this internship I met people from many different countries and all my work was in English so it was also a very good opportunity to improve my English level.

1 ACKNOLEDGEMENTS

First, I want to thank Janlecy Alferes, my supervisor during this project, for her welcome, her advice and guidance and for her good humour. I want to thank Peter Vanrolleghem, the director of the research group, for hiring me for this internship. I also would like Tobias Kraft my coworker and friend for his advice, help an dall the good moment with him during this internship. Besides, I would like to thank Michel Bisping the responsible of laboratory for his help and advice about laboratory analyzes. Also, I would like to thank Sylvie Leduc for her help. Finally, I would thank the technician from WWTP for their availability and help.

2 PRESENTATION

2.1 Laval University

I did my internship in Laval University, Québec city. It's the North America's oldest and biggest French-language university. The Laval University was created in 1633.

Some points of interest::

- More than 420 programs
- Renowned mobility and exchange programs
- 5 profiles: sustainable development, entrepreneurial, international, distinction and research
- Custom, continuing, and distance education programs
- Some 750 partnership agreements with some 525 universities in nearly 70 countries
- A library of over 6 millions documents
- Nearly 40,000 students
- Nearly 4,800 international students
- Some 250 student associations
- $300 million in annual research funding
- 251 centers, chairs, institutes and research groups
- Specialize in many different subject: in optics, photonics and lasers, geomatics, genomics, environmental, older studies, etc…

2.2 model*EAU* research group

model*EAU* is the research team built around the Canada Research Chair on Water Quality Modelling that is held by Peter Vanrolleghem since February 2006. Ten graduate students, three postdocs and two research assistants carry out multifaceted studies in which models are the central ingredient. The research focus is mainly methodological, looking at data collection, data quality evaluation, development of new models and improved modelling approaches, model-based optimization and supporting software.

2.3 mon*EAU* project

Nowadays, on-line sensors are largely used for water quality monitoring of different water bodies to reach different goals. Data acquisition systems can provide high measuring frequencies allowing better description of the dynamics in reactive water bodies (river, combined sewer, etc.) compared to grab or composite samples. Due to the challenging measurements conditions in water environments a large amount of data is produced with uncertain quality. Manual data validation is very tedious and inefficient Therefore, automatic data quality assessment tools (ADQATs) are necessary to validate time series and to use them for their meant application. In that sense, poor quality data could drastically affect the results of their application, namely water quality models, WWTP control rules, etc.

In this project, ADQATs are being developed and applied to real cases to evaluate their performance in terms of producing good experimental data quality.

During this summer the interest is to provide good data that can be used to describe the behaviour of several elements in the process, since the sewer until the first decantation at the WWTP during the dry weather.

We were three persons implied in this project during the summer period, our supervisor Janelcy Alferes Castano and two internships Tobias Kraft and me, Maxime Roussel.

This online station very precise and able to measure many characteristic of water is very interesting to be used in management of treatment plant, to analyze of sewer or to make a study like a modeling.

3 GOALS

I was very interested by the mon*EAU* project because my missions were diversified and the online sensors used during the project will be really implemented and useful in the future in water engineering.

I had different tasks during my 19 weeks internship:

1. Testing of different sensors used by the mon*EAU* station in regards to the ISO standart 15839.
2. Installation and configuration of three mon*EAU* station.
3. Maintain the stations (cleaning and controlling)
4. Collecting of data from the three station and analyze it

4 TESTING OF SENSORS

4.1 Context

The first goal of the internship was to test the new sensors which are in the new stations monEAU. I tested the first sensor with Tobias Kraft, my coworker; it was the Tetracon 700 IQ, aconductivity sensor. Tobias wrote the report for this first testing and I will present here the test of the second one that I tested, the Visoturb 700 IQ, aturbidity sensor.

Turbidity is the cloudiness or haziness of a fluid caused by large numbers of individual particles that are generally invisible to the naked eye, similar to smoke in air. The measurement of turbidity is a key test of water quality.

4.2 Visoturb 700 IQ

VisoTurb® is a digital optical sensor from the WTW brand. It is used with the IQ sensor terminal 2020 XT.Its range or application includes clean water, wastewater or raining water.

Measurement principle: VisoTurb uses the nephelometric principle. Based on this principle, scattered light is measured at an angle of 90 degrees. This method is ideal for low and medium range turbidity up to 4000 FNU (formazin nephelometric Unit). In compliance with EN 27027 and ISO 7027, infrared light using a wavelength of 860 nm. Since this wavelength is outside of the visible range, sample discoloration does not affect measurements.

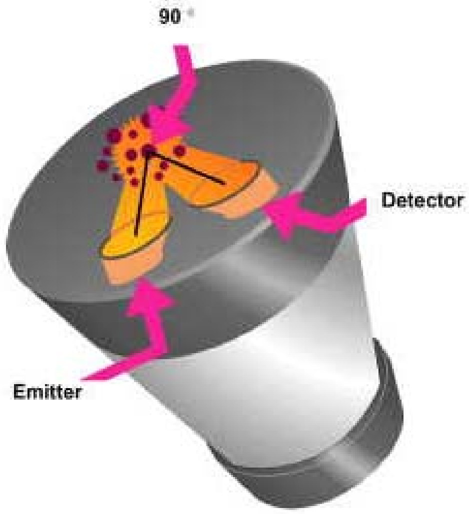

Figure 1: turbidity sensor principle

The Visoturb® is a rugged sensor with a measuring range from 0.05 to 4000 FNUs. Ideal sensor for the quantitative measurement of remaining undissolved solids at the effluent of a treatment plant.

4.3 Testing protocol

We tested the sensors in regards to the standard ISO 15839:2003 'Water quality – On-line sensors/analyzing equipment for water - Specifications and performance tests' it's a guide for testing water quality sensors on their performance characteristics. This protocol consists of a part of laboratory tests and of a part of tests in the field. All the laboratory tests are conducted with seven solutions covering the working range of the sensor. Those seven solutions are 5, 20, 35, 50, 65, 80 and 95 % of the working range.

The following characteristics can be determined by the laboratory tests:

- Response time, delay time, rise time and fall time
- Linearity, coefficient of variation, limit of detection, limit of quantification, repeatability, lowest detectable change, bias, short-term drift, day-to-day repeatability
- Memory effect
- Interferences
- Environmental and operating conditions

The following characteristics can be determined by the test in field conditions:

- Response time, delay time, rise time and fall time
- Bias based on differences
- Long-term drift
- Availability
- Up-time

4.4 Laboratory testing

For testing the Visoturb 700 IQ sensors only the laboratory tests were conducted (without the characteristics 'interference' and 'environmental and operating conditions').

The actual measuring range of VisoTurb700 IQ is between 0 NTU to 400 NTU. Eight calibration solutions were prepared for a maximum turbidity value of 800 NTU which is within the range of typical wastewater. Eight calibration solutions, as shown in Table 1, were prepared using high-purity, deionized, co2-free water and cutting oil.

Table 1: Calibration solutions

Tests of the Visoturb700IQ sensor

Percentage of the working range [%]	Solution Value [NTU]
5	20
20	80
35	140
50	200
65	260
80	320
95	380
200	800

These solutions were prepared with cutting oil having as big advantage thatthe price for all solutions is 2$. However, as disadvantage the turbidity tend to increase within a long time (24h) so we needed to adjust the solutions each day. That mean the solutions didn't have exactly the same turbidity day after day so we couldn't do "short term drift" and "day to day repeatability" test.

4.4.1 Response time, delay time, rise and fall time

For determining the response, delay, rise and fall time the calibration solutions at 20% and 80% of the working range were used by doing the following steps:

1. The sensor was immersed in the 20% solution until the signal was stable.
2. The sensor was immersed in the 80% solution.
3. Three response time later the sensor was immersed again in the 20% solution

This procedure was repeated six times and every time recorded. The definitions and calculations are explain in the appendix part section 11.1

4.4.2 Linearity, Coefficient of variation, limit of detection, limit of quantification, repeatability, lowest detectable change, bias, short-term drift and day-to-day repeatability

For carrying out this set of tests the calibration solutions at 0 (blank), 5, 20, 35 50, 65, 80 and 90% of the working range were used. The sensor was exposed to each of the solutions with the blank solution in between. For every concentration six measurements were taken which were scheduled as shown in Table 3. After the signal became stable a measurement was carried out. The calculations for each characteristic are in accordance to Table 2. All definitions and calculations are in section 11.2

Table 2: Use of measurements on scheduling

i	x_i [%]	Determinant level used for	To be measured
1	5	LOD, LOQ	On the same day separated by blanks
2	20	Repeatability, LDC, bias	On the same day separated by blanks
3	35	Day-to-day repeatability	On different days
4	50	Short-term drift	Equally distributed over shortest period between maintenance operations
5	65	Day-to-day repeatability	On different days
6	80	Repeatability, LDC, bias	On the same day separated by blanks
7	95	Linearity check only	On the same day separated by blanks

Table 3: Scheduling of the laboratory tests

i	x_i [%]	Reference NTU	$y_{i,1}$ NTU	$y_{i,2}$ NTU	$y_{i,3}$ NTU	$y_{i,4}$ NTU	$y_{i,5}$ NTU	$y_{i,6}$ NTU
1	5	1	Day 4	Day 4	Day 4	Day 4	Day 4	Day 4
2	20	4	Day 6	Day 6	Day 6	Day 6	Day 6	Day 6
3	35	7	Day 3	Day 4	Day 5	Day 6	Day 7	Day 8
4	50	10	Day 5	Day 5	Day 5	Day 5	Day 5	Day 5
5	65	13	Day 4	Day 4	Day 5	Day 6	Day 7	Day 8
6	80	16	Day 7	Day 7	Day 7	Day 7	Day 7	Day 7
7	95	19	Day 3	Day 3	Day 3	Day 3	Day 3	Day 3

4.4.3 Memory effect

The sensor was exposed to a calibration solution with a determinant value of 200% of the working range for a period equal to five times the response time, and then changed to a 20% calibration solution. Three response times after the changeover, a measurement was carried out. This procedure was repeated six times.

4.5 Results and Discussion

4.5.1 Response time, delay time, rise and fall time

One of the most important characteristic of these sensors is their response time,always around 60s. We need to know that and include this time for well analyze the data. Comparing the Tetracon 700 IQ has almost no response time (<0s). The graphs below show the different results about temporal response for the six VisoTurb 700 IQ that we tested.

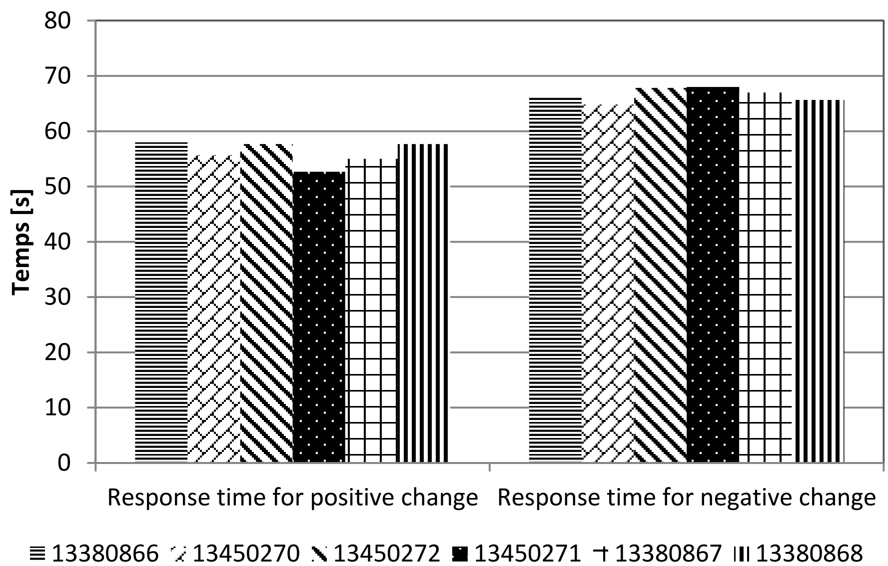

Figure 2: Response time results

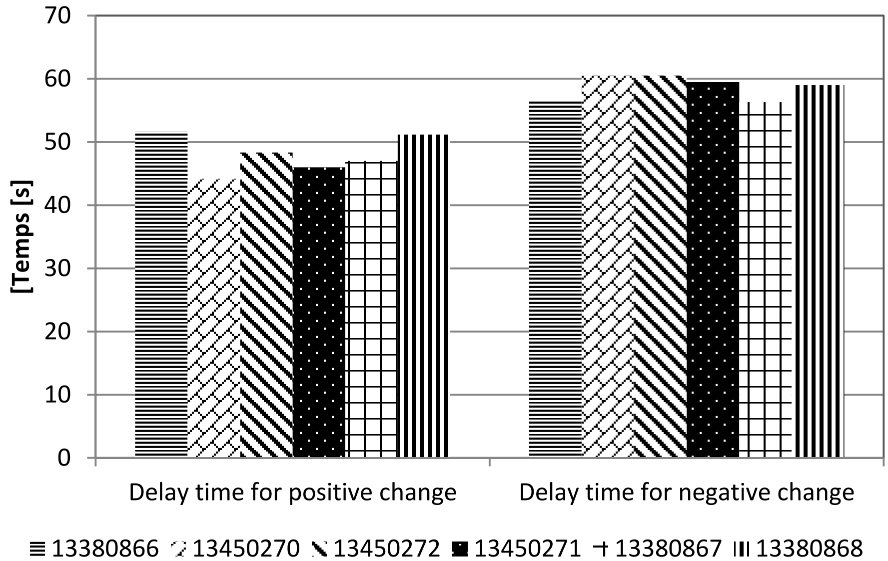

Figure 3: Delay time

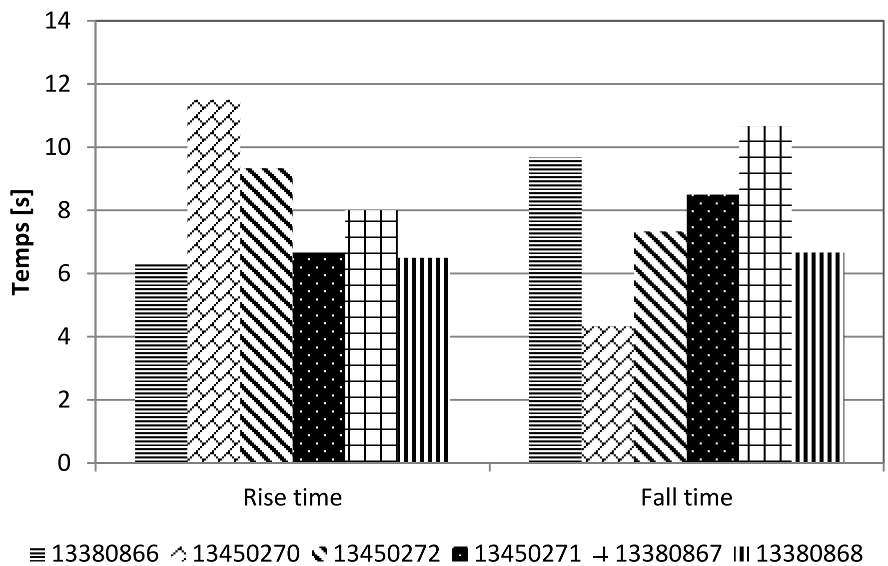

Figure 4: Rise and fall time

These results show three different aspects:

1. The response times are very important (always close to 1min)
2. The temporal characteristic are almost the same for the six sensors
3. Almost all the response time is composed by the delay, The rise time and the fall time are short (<10s)

4.6 Linearity, Coefficient of variation, limit of detection, limit of quantification, repeatability, lowest detectable change, bias, short-term drift and day-to-day repeatability

A summary of all the performance characteristics of each Visoturb 700 IQ sensor is listed in Table 4. Those values were determined following the ISO 15839:2003. In the following subsections those performance characteristics are shown graphically. The measurements results of each Visoturb 700 IQ are in appendix part section 11.4.

Table 4: Characteristics of different VisoTurb700 IQ WTW Turbidity sensor

Performance characteristics	Unit	Sensors Serial number					
		13380866	13450270	13450272	13450271	13380867	13380868
Linearity	-	1.000	0.999	0.999	0.999	1.000	0.999
Coefficient of variation	%	2.455	3.099	3.710	2.307	2.639	2.679
LOQ	NTU	0.605	0.453	5.315	4.290	0.285	1.824
LOD	NTU	2.018	1.508	17.717	14.299	0.950	6.081
Repeatability 20%	NTU	1.385	1.950	0.099	0.651	0.417	3.496
80%	NTU	0.442	0.667	2.737	0.481	1.085	1.072
LDC 20%	NTU	4.155	5.850	0.297	1.952	1.252	10.487
LDC 80%	NTU	1.327	2.000	8.210	1.442	3.254	3.216
Bias 20%	NTU	-0.036	5.787	3.970	-1.114	2.148	5.985
Bias 80%	NTU	3.773	7.054	7.021	-12.190	1.602	4.254
Day-to-day repeatability 35%	NTU	2.742	3.024	3.795	1.587	1.650	1.810
65%	NTU	3.668	4.026	5.621	3.777	4.745	3.623
Response time positive change	s	58.000	55.667	57.667	52.667	55.000	57.667
negative change	s	66.167	64.833	67.833	68.000	67.000	65.667
Delay time for positive change	s	51.667	44.167	48.333	46.000	47.000	51.167
negative change	s	56.500	60.500	60.500	59.500	56.333	59.000
Rise time	s	6.333	11.500	9.333	6.667	8.000	6.500
Fall time	s	9.667	4.333	7.333	8.500	10.667	6.667

4.6.2 Linearity

The linearity of each sensor resulted very high, almost a value of one. So the linearity capacities of all VisoTurb 700IQ are almost perfect. The Tetracon 700 IQ has almost the same result. The Figure 5 below shows the result of linearity test for the 6 VisoTurb that we tested.

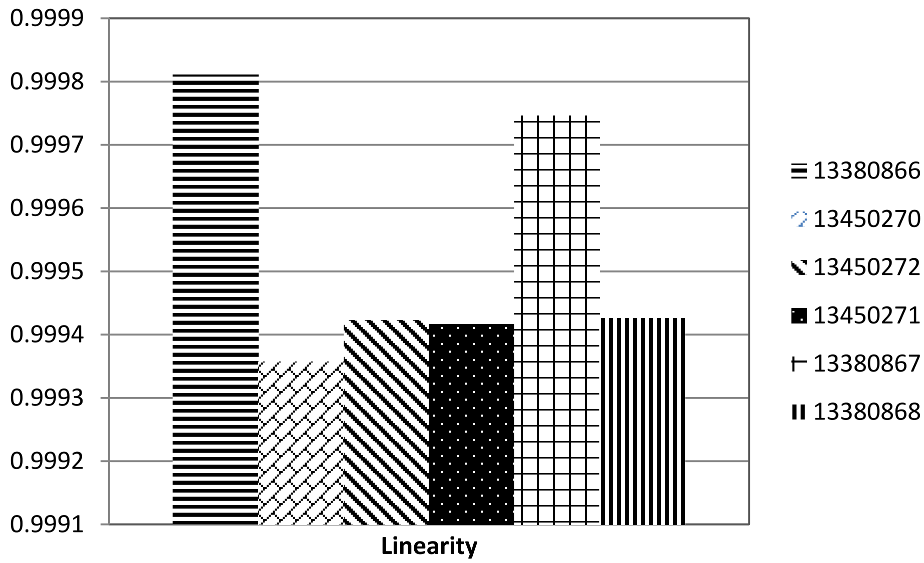

Figure 5: Comparison of linearity of different Visoturb 700 IQ sensors

4.6.3 Coefficient of variation

In the Figure 6 the coefficient of variation of each Visoturb 700 IQ is displayed. The values are between 2.307 to 3.710%. Comparing the mean of coefficient of variation for the conductivity sensors TetraCon 700 IQ, that were around 4.105%, the VisoTurb have a better behaviour in this characteristic.

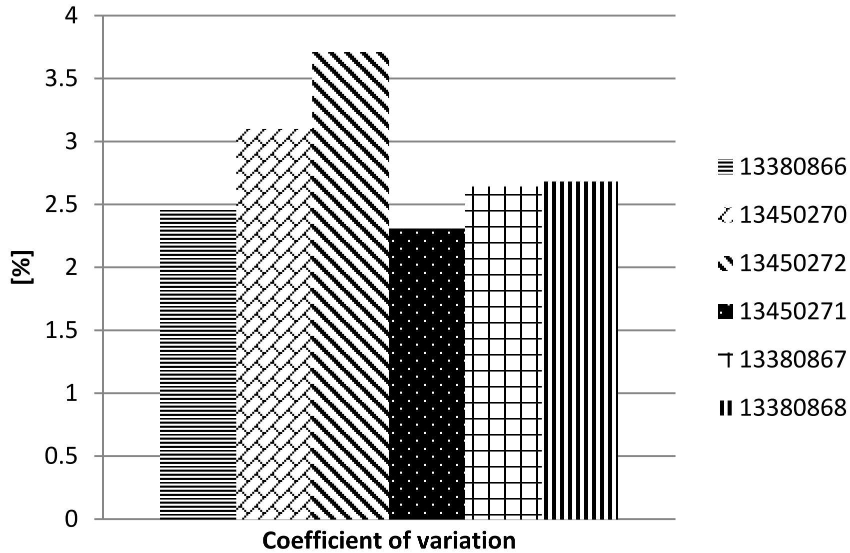

Figure 6: Comparison of coefficient of variation of different Visoturb 700 IQ sensors

4.6.4 *Limit of detection and quantification, repeatability, lowest detectable change and day-to-day repeatability*

The limit of detection and quantification, repeatability, lowest detectable change and day-to-day repeatability are in the same section because they are all based on calculations with the standard deviation of the measurements.

In Figure 7 the limit of detection and the limit of quantification are displayed for all different Visoturb 700 IQ sensors. Both characteristics have the same shape but different values. This is because both are calculated by the standard deviation of 5% measurment. The values of the limit of quantification are higher than the ones of the limit of detection.

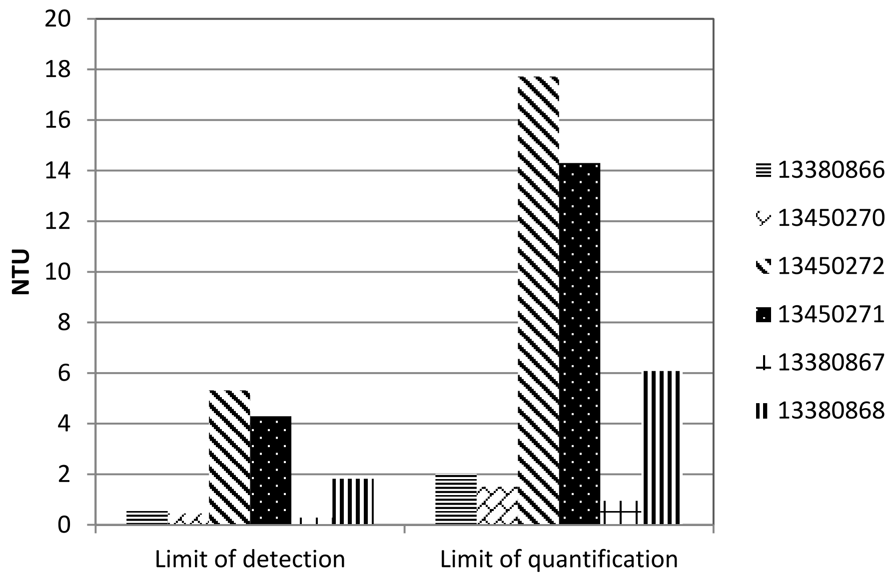

Figure 7: Comparison of limit of detection and quantification

In Figure 8 a comparison of the repeatability at 20 and 80% of the working range of the six different VisoTurb 700 IQ sensors are shown and Figure 9 illustrates the comparison of the lowest detectable change at 20 and 80% of the working range of same sensors. The shapes in those two figures are the same because the repeatability is calculated by the standard deviation and the lowest detectable change is calculated by 3 times the standard deviation.

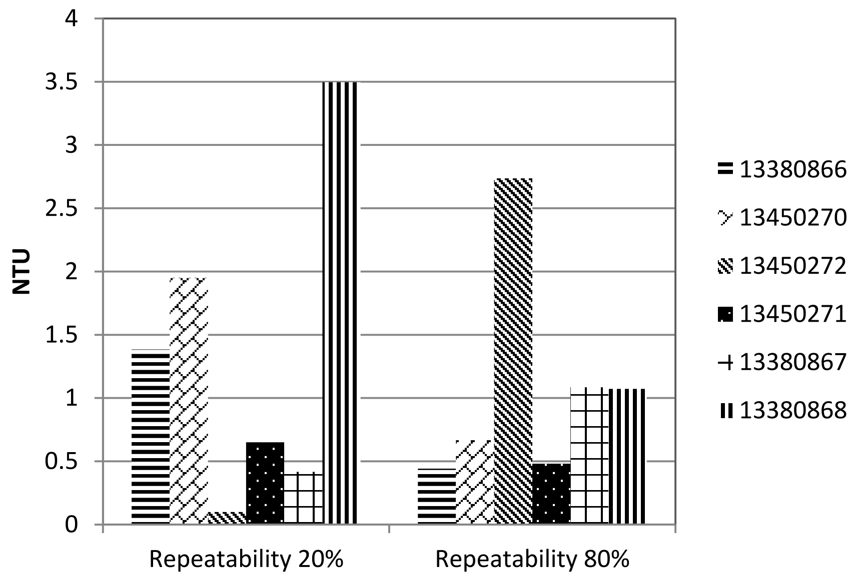

Figure 8:Comparison of repeatability at 20% and 80% of the working range

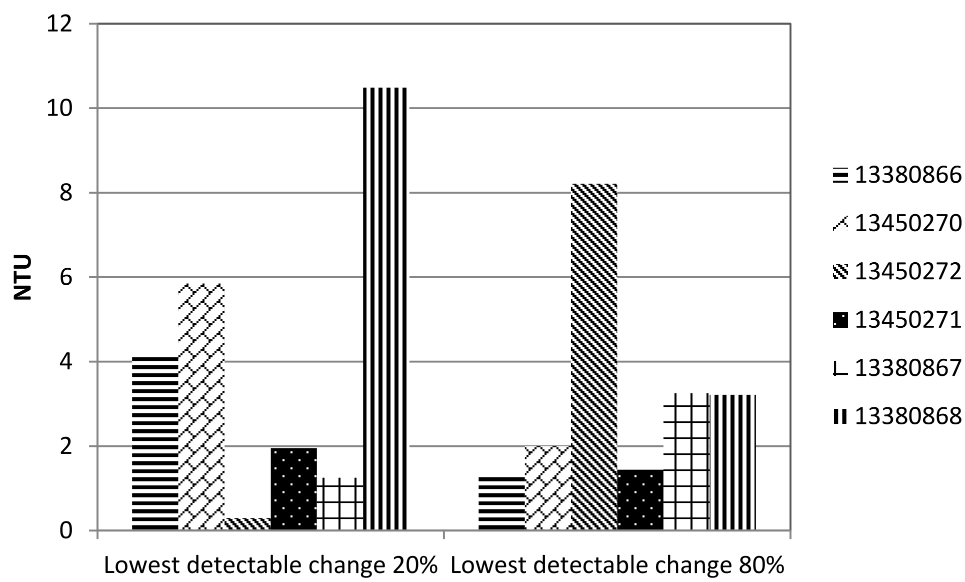

Figure 9: Comparison of lowest detectable change at 20% and 80% of the working range

4.6.6 Bias

Figure 10 shows the comparison of the bias at 20 and 80% of the working range of the different turbidity sensors tested. The bias is calculated by difference between measurement of the sensor and the reference measurement. Both measurements are with uncertainties. All the sensors have a positive bias except the number 13450271 which has negative bias.

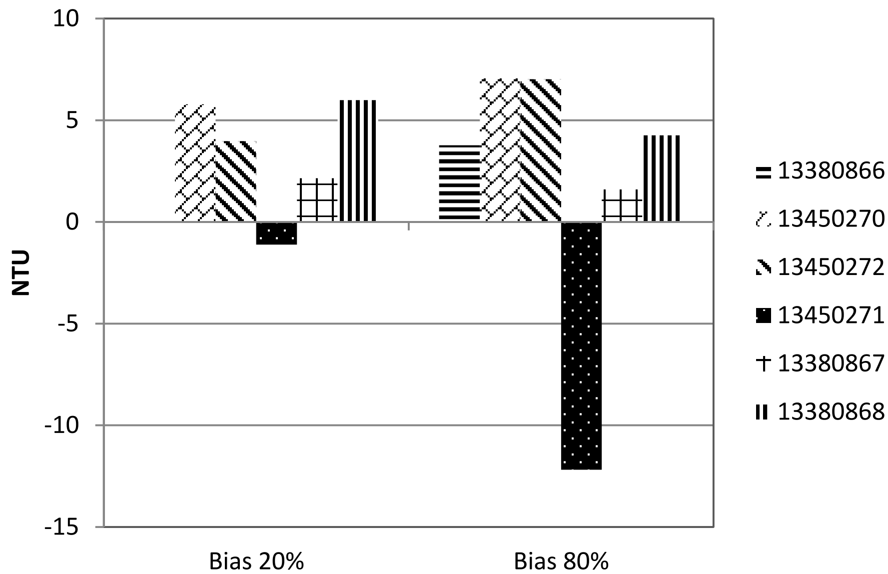

Figure 10: Comparison of bias at 20% and 80%

4.7 Memory effect

In regard to standard ISO 15839:2003 there is a memory effect when the memory effect value is bigger than the lowest detectable change 20%. The Figure 11 below shows the different memory effect measured for the five VisoTurb 700 IQ at right and the $LDC_{20\%}$ at left. Only the n°13450272 has a small memory effect. I didn't test the memory effect for the n°13380866 because it was already installed in a field when I did these tests.

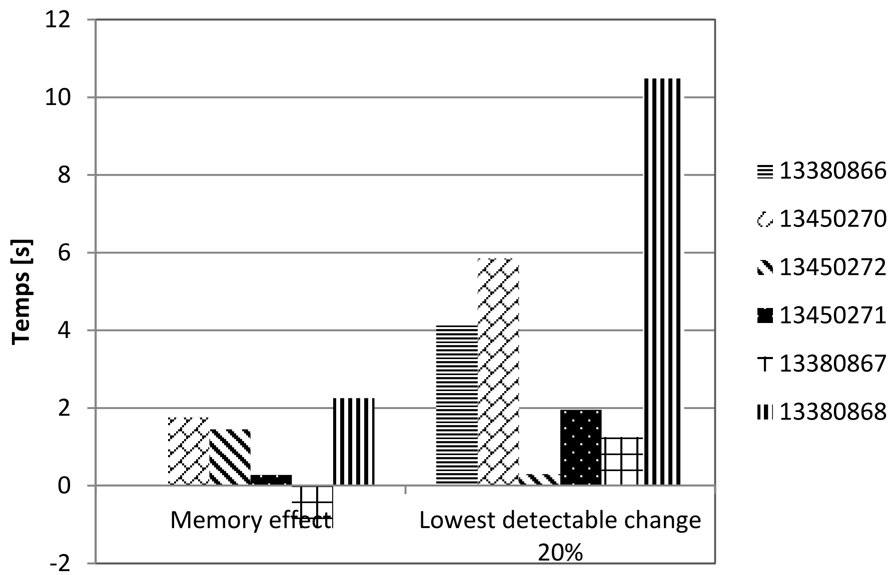

Figure 11: Comparison of memory effect

4.8 Conclusion

Once of the most important a characteristic of these sensors is their response time, it was always close to 60s and that relatively long. We need to know that and include this time for analyze the data well.

The linearity was very good for all the sensors, all close to the unit.

All the other different sources of uncertainties (repeatability, detectable change, etc.) are between -10 and 10 NTU. These margins of errors represent 0.25% of the working range.

These sensors are totally appropriate to work for studying the turbidity of water and wastewater

5 INSTALLATION AND CONFIGURATION

The second goal of my internship in model*EAU* was to install and configure three mon*EAU* stations.

5.1 Location

The first station was installed at the entrance of the primary clarifier in the Wastewater Treatment Plant of Beauport, Québec, QC. The second one was installed in the sewer at the Saint Sacrement network. The last one was installed in the entrance of a grit chamber. The Figure 12 shows the main sewer of Québec city and the place where the stations were installed.

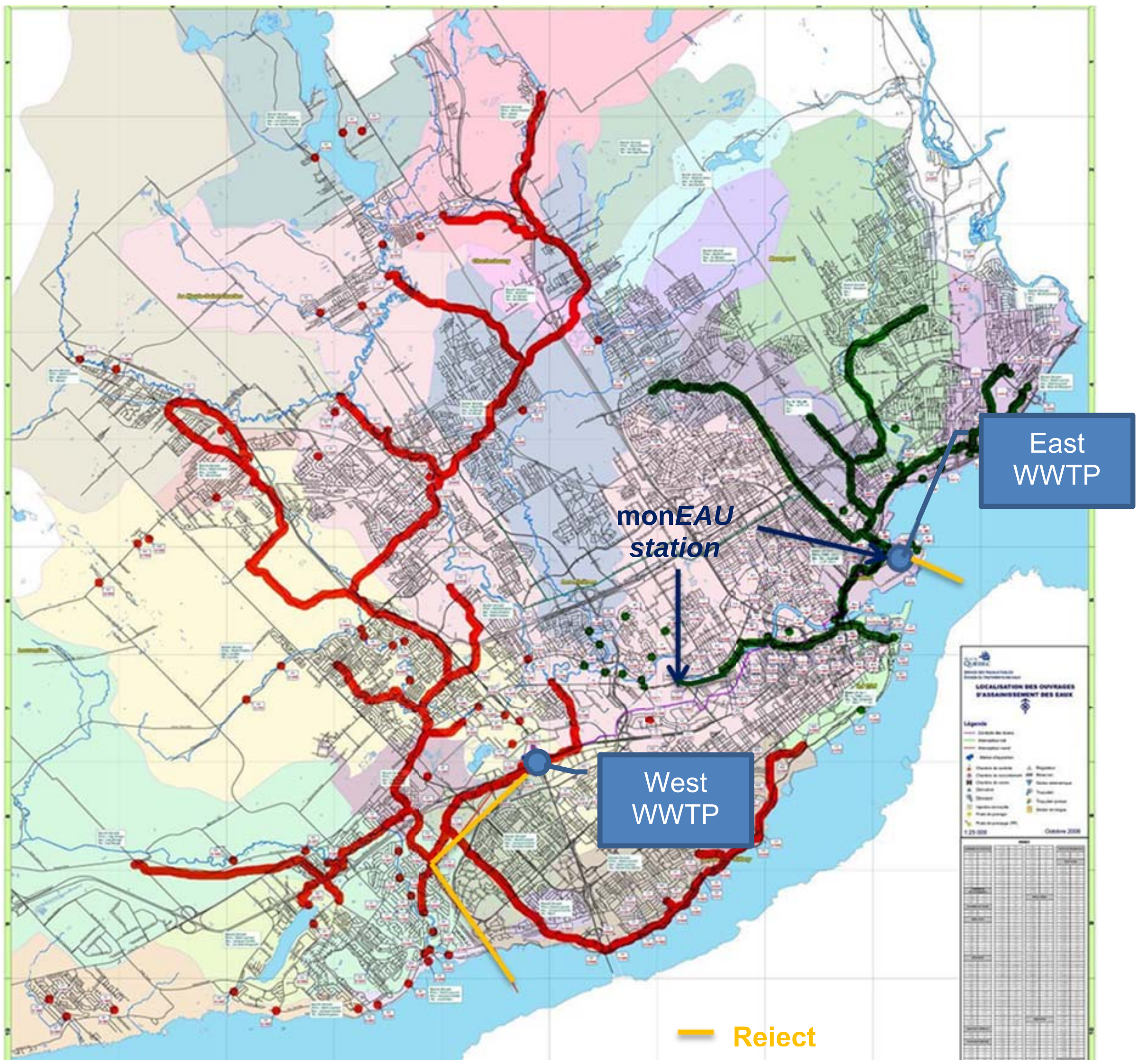

Figure 12: Main sewer of Québec city

The Figure 13: Detailed plan of east WWTP Beauport Québec city shows the different parts of the WWTP of Québec city and the place where the mon*EAU* station are installed.

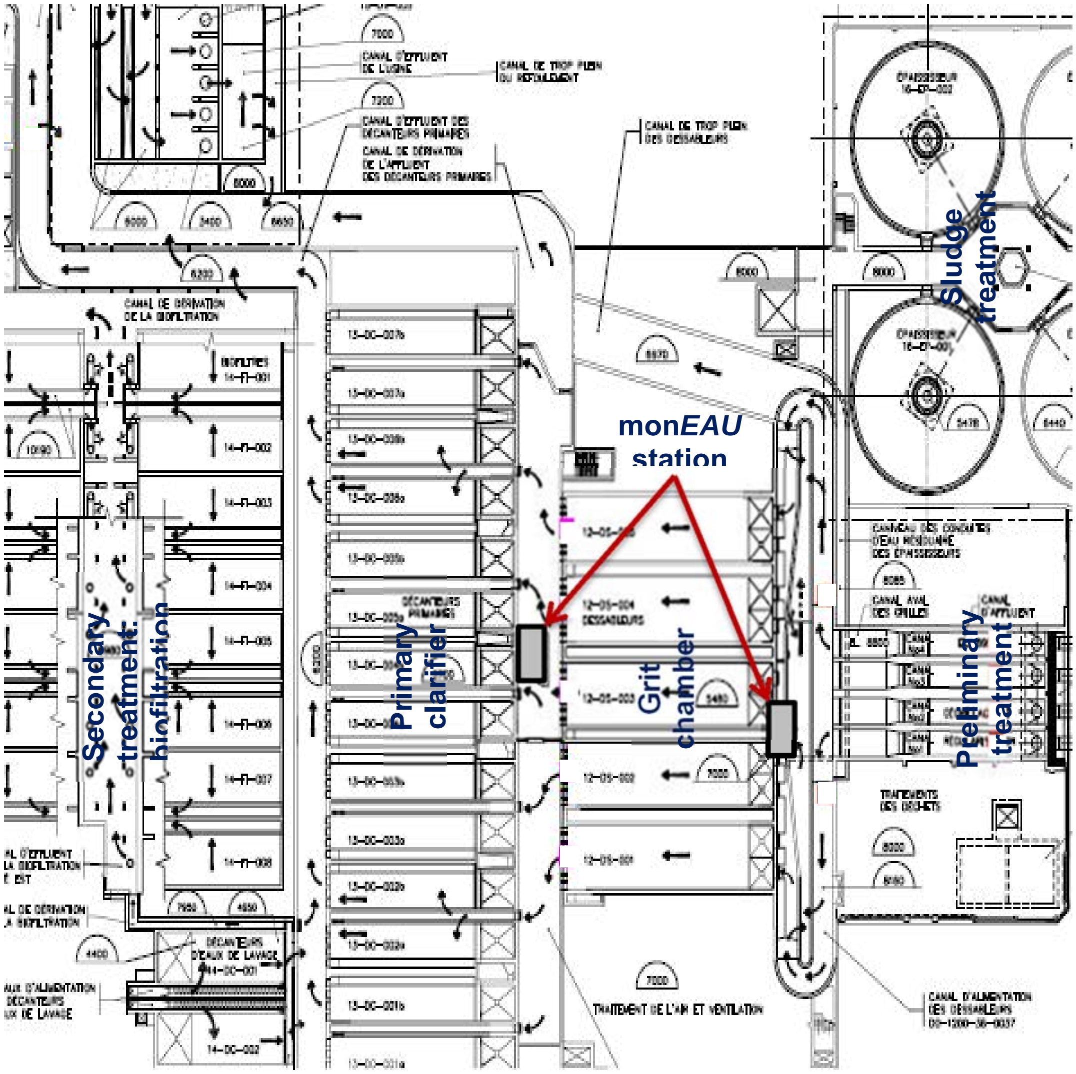

Figure 13: Detailed plan of east WWTP Beauport Québec city

5.2 Installation

The three stations were installed at the points shown in last section. The structures where the sensors are fixed were made by the technicians from the WWTP following the recommendations given by the monEAU group.

5.2.1 Entrance of primary clarifier

The first station was installed at the entrance of the primary clarifier.

Figure 14: Primary clarifier installation n°1

The supports are made of steel rod where the sensors are attached and immerse in the wastewater. This rod is fixed on the floor by screws.

Figure 15: Primary clarifier installation n°2

5.2.3 Sewer Saint Sacrement

The second station was installed in the sewer at saint Sacrement. The support for the sensors is guided by a rail and moved by a cable and a crank. The support need to be very strong because the flow in the sewer is very powerful.

Figure 16: Sewer Saint Sacrement installation n°1

The Figure 17 below shows the support system when the sensors are outside.

Figure 17: Sewer Saint Sacrement installation n°2

5.2.5 Entrance of grit chamber

The third station was installed in the entrance of the grit chamber. The Figure 18 shows the sensor support. The system to remove the sensor out of the waste water is moved by electric hoist. The system is strong because the flow at this point is so powerful.

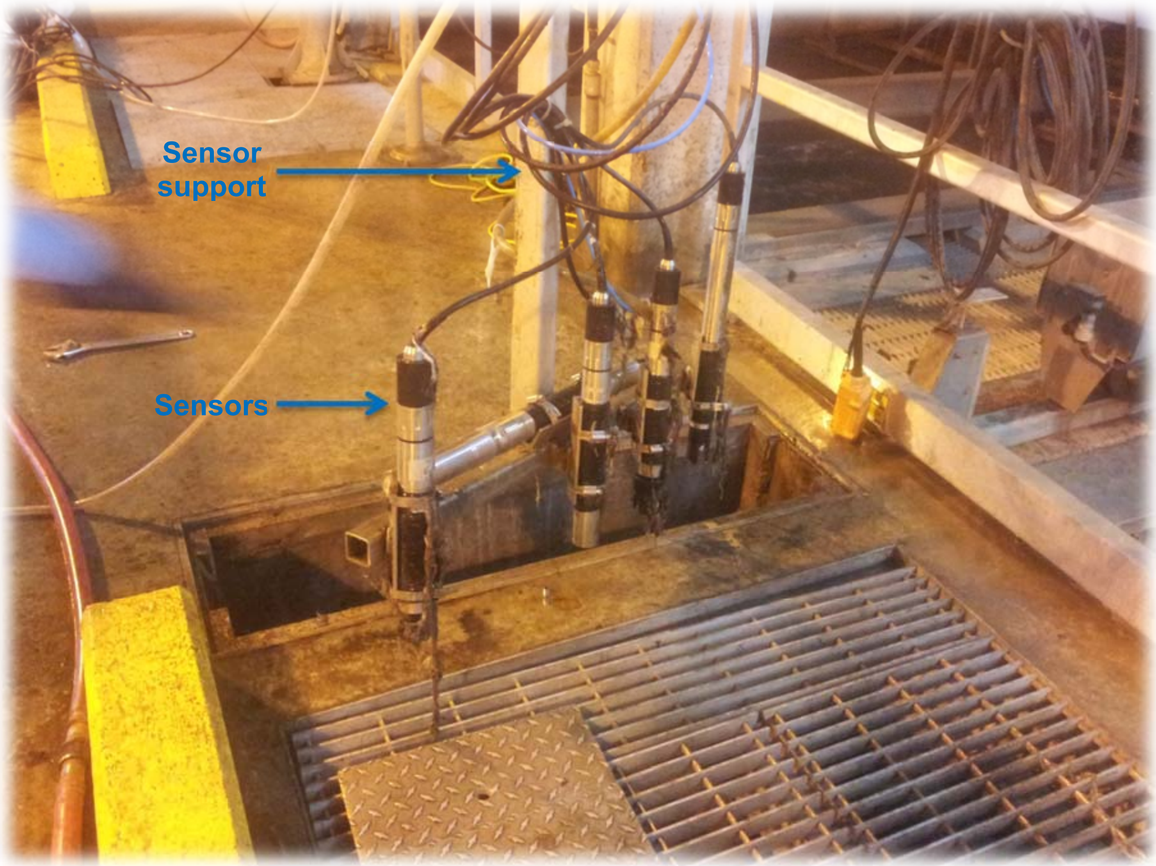

Figure 18: Entrance of grit chamber installation

5.4 Components of the monEAU stations

5.4.1 Station

The Figure 19 shows the different components of mon*EAU* station.

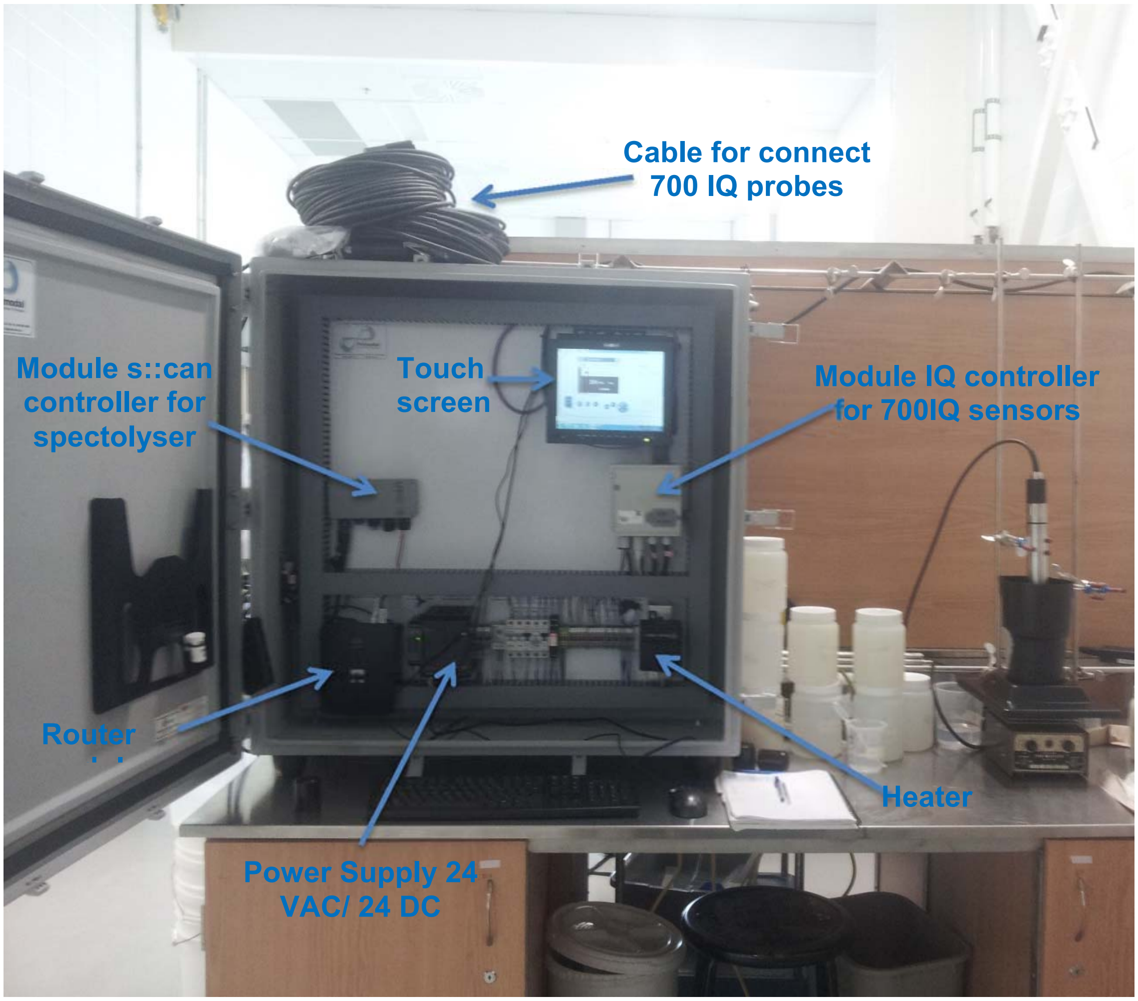

Figure 19: mon*EAU* station components

The three stations have the same configuration and the same set of sensors. There are 5 different sensors listed and presented below.

5.4.2 Sensors

Presentation of all sensors used during this summer with the mon*EAU* station

Visoturb® 700 IQ:

Digital VisoTurb® optical turbidity and total suspended solids sensor. It is used with the IQ sensor terminal 2020 XT. Application ranges from raining water to wastewater

Measurement principle: VisoTurb uses the nephelometric principle show by the Figure 20. Using this principle, scattered light is measured at an angle of 90 degrees. This method is ideal for low and medium range turbidity up to 4000 FNU (formazin nephelometric Unit). In compliance with EN 27027 and ISO 7027, infrared light using a wavelength of 860 nm. Since this wavelength is outside of the visible range, sample discoloration does not affect measurements.

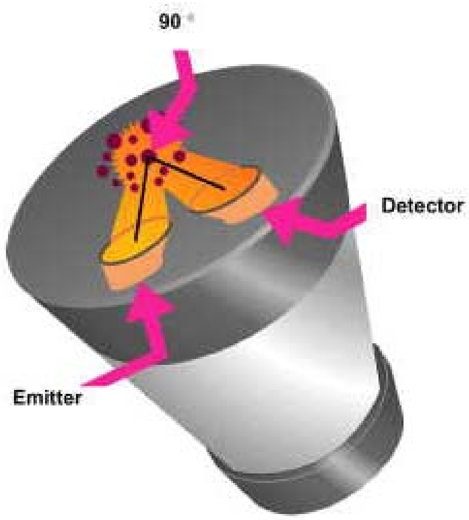

Figure 20: Turbidity sensor principle

The Visoturb® is a rugged sensor with a measuring range from 0.05 to 4000 FNUs. Ideal sensor for the quantitative measurement of remaining undissolved solids at the effluent of a treatment plant.

Sensolyt® 700 IQ:

Digital pH/ORP sensor for various SensoLyt® electrodes (SEA/DWA/ECA/PtA) for use with the IQ SensorNet terminals 2020 XT. Built-in pre-amplifier and temperature sensor with SensCheck function to monitor the sensor.

Characteristics:

- provide pre-amplification of the electrode signal
- digital sensor stores calibration value
- automatic temperature compensation
- SensCheck function to monitor for sensor functionality
- rugged protection
- electrodes can easily be replaced without tools
- electrodes can be removed and calibrated in the lab if necessary or simply calibrate on the field

Figure 21: SensoLyt® 700 IQ

We used ECA electrode for pH and Pta for ORP.

ECA Characteristics:

This combination pH electrode has a single pin-hole diaphragm and a gel electrolyte. With its long-term stability it provides an economical solution, particularly in most wastewater facilities.

Functioning of pH electrodes:

Most often used pH electrodes are glass electrodes. Typical model is made of glass tube ended with small glass bubble. Inside of the electrode is usually filled with buffered solution of chlorides in which silver wire covered with silver chloride is immersed. pH of internal solution varies - for example it can be 1.0 (0.1M HCl) or 7.0 (different buffers used by different producers).

Active part of the electrode is the glass bubble. While tube has strong and thick walls, bubble is made to be as thin as possible. Surface of the glass is protonated by both internal and external solution till equilibrium is achieved. Both sides of the glass are charged by the adsorbed protons, this charge is responsible for potential difference. This potential in turn is described by the Nernst equation and is directly proportional to the pH difference between solutions on both sides of the glass.

The majority of pH electrodes available commercially are combination electrodes that have both glass H^+ ion sensitive electrode and additional reference electrode conveniently placed in one housing. For some specific applications separate pH electrodes and reference electrodes are still used - they allow higher precision needed sometimes for research purposes. In most cases combination electrodes are precise enough and much more convenient to use.

Construction of combination electrode is in large part defined by the processes that must take place when measuring pH. We need to measure difference of potentials between sides of glass in the glass electrode. To do so we need a closed circuit.

Circuit is closed through the solutions - internal and external - and the pH meter. However, for correct and stable results of measurements reference electrode must be isolated from the solution so that they will not crosscontaminate - and it is not an easy task to connect and isolate two solutions at the same time.

Connection is made through a small hole in the electrode body. This hole is blocked by porous membrane, or ceramic (asbestos in older models) wick. Internal solution flows very slowly through the junction, thus such electrodes are called flowing electrodes. To slow down the leaking, in gel electrodes internal solution is gelled.

The Figure 22 below shows how a combination electrode is made.

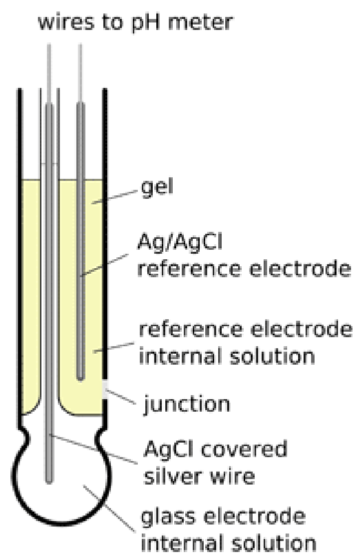

Figure 22: pH elctrode explanation

Pta characteristic:

This ORP electrode is also fitted with a pinhole diaphragm, and is primarily recommended for applications in heavily contaminated wastewater.

Used for municipal and industrial sewage, emulsions and suspensions, media containing proteins and sulfides. The working range of Pta electrode is -2000 to 2000 mV.

Functioning of ORP elctrodes:

The system is close to an pH electrode. When you put an ORP electrode in the water there are an exchange of ion between the oxidized state and the reduced state of an electrolyte. The tension in result of this exchange is the Oxydo Reduction Potential.

Tetracon 700 IQ:

Digital conductivity sensor TetraCon® is used with the IQ SensorNet terminals 2020 XT. Built-in temperature sensor and 4 conductivity electrodes. Tetracon are especially suitable for wastewater. Due to the 4-electrode measuring technique, severe influences from polarization effects are eliminated, resulting in improved accuracy. The cell geometry makes it impervious to fouling, and the abrasion resistant carbon electrodes are easy to clean.

With the TetraCon 4-electrode design, two separate electrode pairs are used whereby the currentless voltage electrodes produce a stable and constant reference potential. The voltage drop at the current electrodes is regulated. The advantage is a more stable reading even in high conductivity environments.

TetraCon 700 IQ sensors:

- 4-electrode design
- extremely robust and durable
- large measuring range with a single cell
- highly resistant to fouling

The Tetracon 700 IQ is a rugged sensor with a measuring range from 10 to 500 mS/cm.

Functioning:

The conductivity is the ability of solution to conduct electrical current. There is an electrical current flowing between two electrodes in the solution. And the probe calculates the facility for the current to switch from one electrode to the other. The conductivity is affect by the temperature of the solution then there is a thermometer include in the Tetracon 700 IQ

Figure 23: Tetracon 700 IQ

Varion^{plus} 700 IQ:

Digital VARiON® Plus ammonium, nitrate and potassium ISE sensor for use with the IQ SensorNet terminals 2020 XT.

The efficient control of Nitrogen in wastewater systems is possible by making those measurements directly in the wastewater process. The direct ISE measuring technology with the VARiON sensor enables optimization of a plant in respect to process efficiency and energy consumption.

Figure 24: Varion^{plus} 700 IQ

Functioning:

The Varion^{plus} 700 IQ is made with selective electrode. This kind of electrode has special membrane where just one kind of ion can adhere. Consequently there a specific potential on the membrane surface. The potential is measured by the sensor to determine the concentration of the ion.

Working Range:

-NH4-N: 1 to 1000 mg/L

- NO3-N: 1 to 1000 mg/L

- K^+: 1 to 1000 mg/L

S::can Spectrolyser:

spectro::lyser™ UV monitors depending on the application an individual selection of: NO3-N, COD, BOD, TOC, DOC, UV254, NO2-N, BTX, AOC, fingerprints and spectral alarms, temperature and pressure

Functioning

Spectrometer probes work according to the principle of UV-Vis spectrometry. Substances contained in the medium to be measured weaken a light beam that moves through this medium. The light beam is emitted by a lamp, and after contacts with the medium its intensity is measured by a detector over a range of wavelengths. Each molecule of a dissolved substance absorbs radiation at certain and known wavelength. The concentration of substances contained determines the size of the absorption of the sample - the higher the concentration of a certain substance, the more it will weaken the light beam. The sensor has an auto clean system with pressure air.

Figure 25: Spectrolyser s::can

5.6

5.7 Maintainence

Two times per week we need two remove all the sensors out of the waste water to clean it. There are two kind of dirtiness to be removed, first one mud and solid part and second one the small particules and/or biofilm. For the mud and the solid part we used pressure water. For the biofilm, we used a special cleaning product provided by s::can for the spectro::lyser or a 3% HCl solution together with soft paper

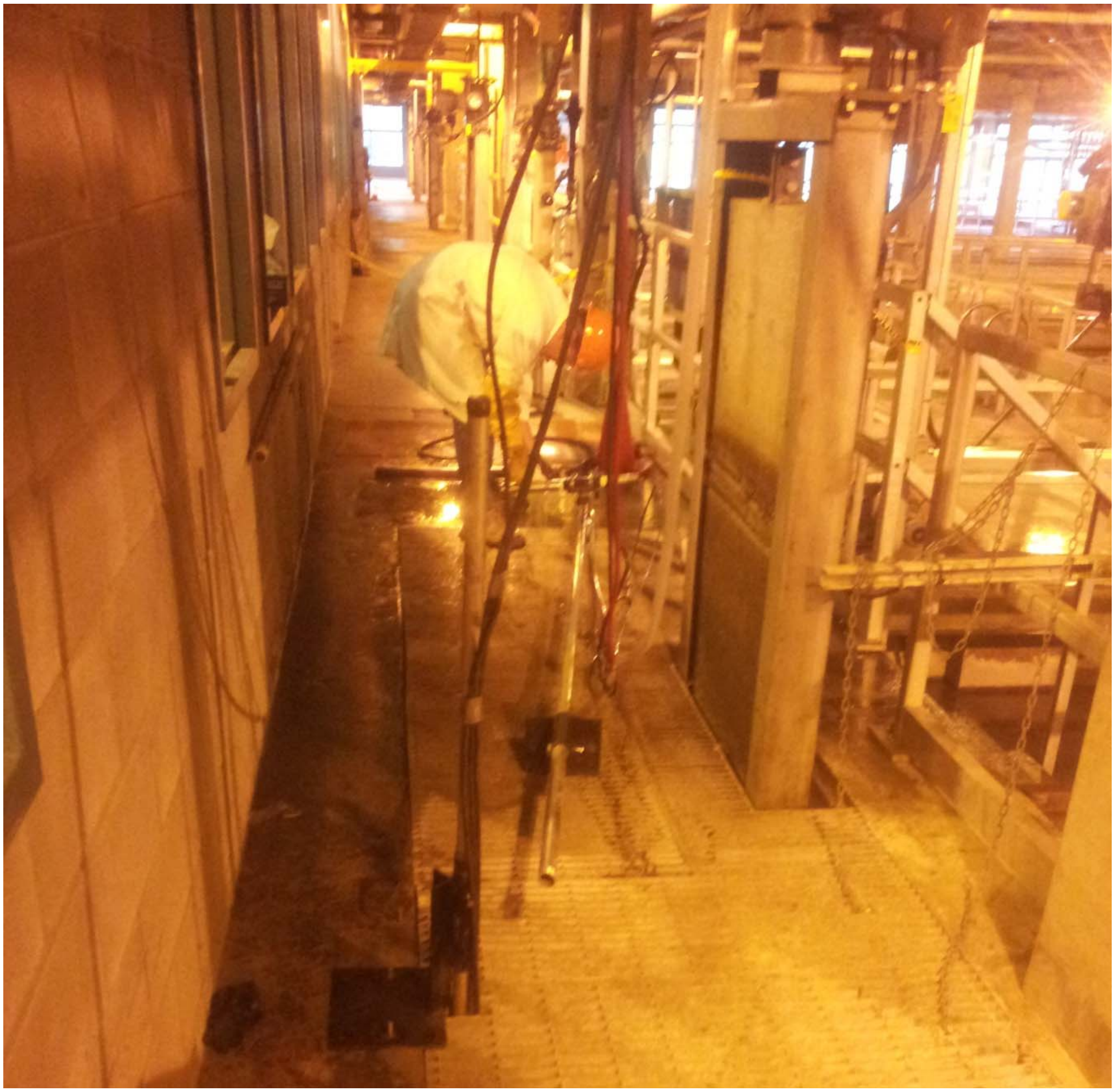

Figure 26: Cleaning sensors

6 CONTROLE

To control the values provided by the sensors, we took sample of wastewater at the three installations. We analyzed these samples in laboratory at the University. After we compared the values from the station and the result of laboratory analyzes and we could see which sensor need a correction and which one give a good value. The Figure 26 shows the laboratory of water engineering at University Laval where we did the analyzes.

Figure 27: Laboratory testing

Error! Reference source not found. below schow the result of control realized on September 16 at the stion installed in the entrance of grit chamber.

Table 5:: Control of monEAU data

Characteristic	monEAU data	Laboratory results
Turbidity	400	432.67
K	36	9.20
N-NH4	15	21.2
pH	7.3	7.41
Conductivity	780	765

7 DATA ANALYSE

Analyze of data from mon*EAU* station is realized with result of analyze campaign of water in laboratory. These analyses campaigns consist to take sample each hour during 24 hours at the three installations and analyze it in laboratory with classic method. After that we can compare the result and the data from monEAU station. We compare the value and the pattern of each parameter. There are, in all data from mon*EAU* station, a time without value, it was a cleaning time.

7.1 Grit chamber

The Figure 28 and Figure 29 below show the laboratory results and the data from mon*EAU* station installed at the entrance of the grit chamber.

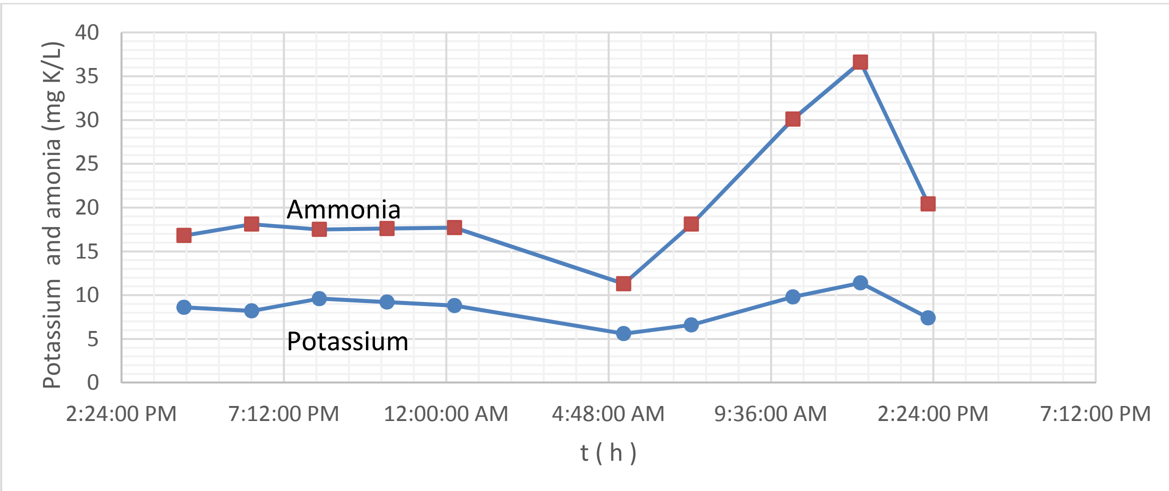

Figure 28: Results analyse campaign, K et N-NH4, entrance of grit chamber

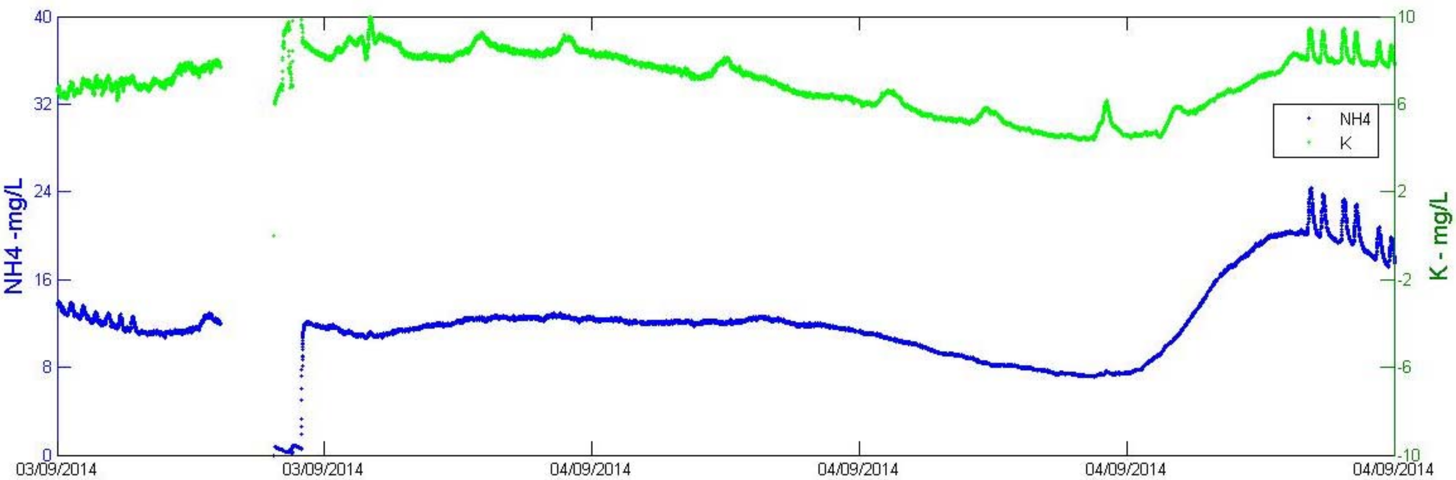

Figure 29: Data from mon*EAU* station, K and N-NH4, entrance of grit chamber

The pattern seems good there an increasing at the end in both place but the values are really bad for the K and not perfect for the $N\text{-}NH_4$. We need to check the Varion^{plus} at this place.

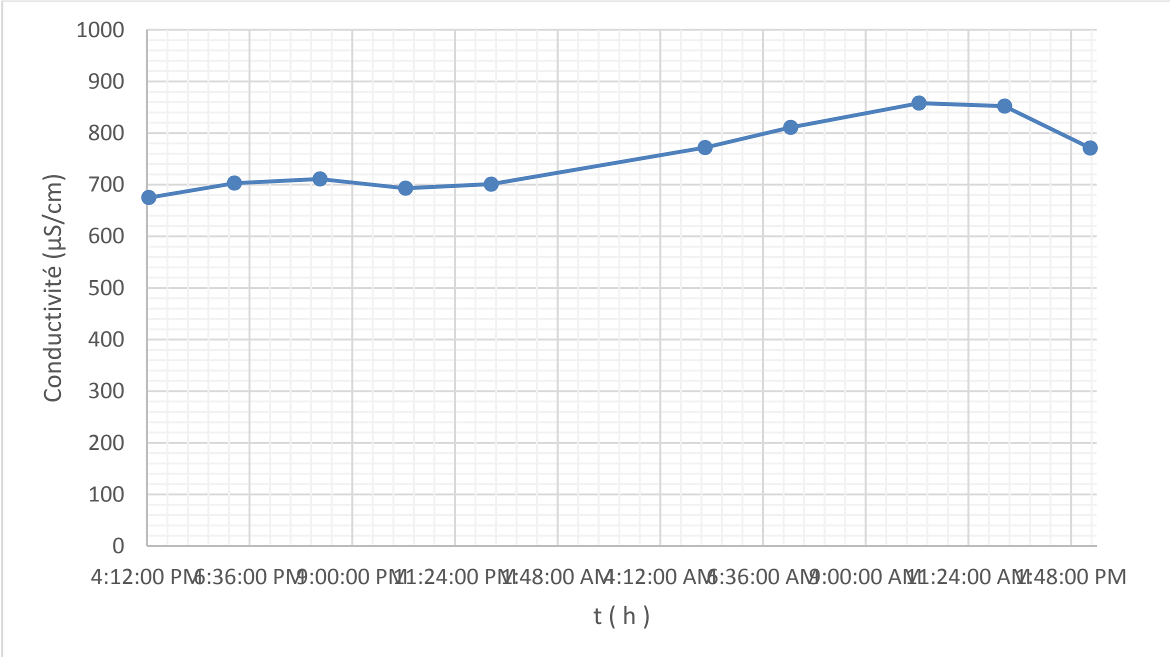

Figure 30: Results analyse campaign, conductivity, entrance of grit chamber

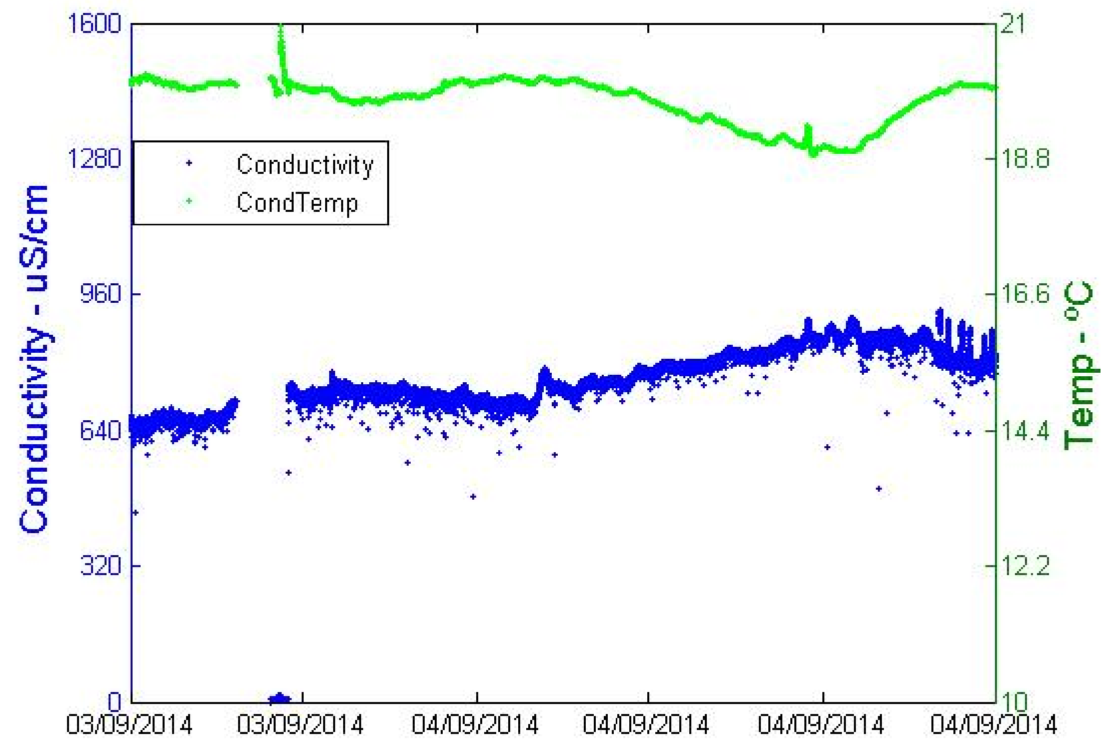

Figure 31: Data from monEAU station, conductivity, entrance of primary clarifier

For this sensor, the Tetracon 700 IQ the value and the pattern are similar in laboratory analyze and in the data from the station. We just have some outsider value and noise.

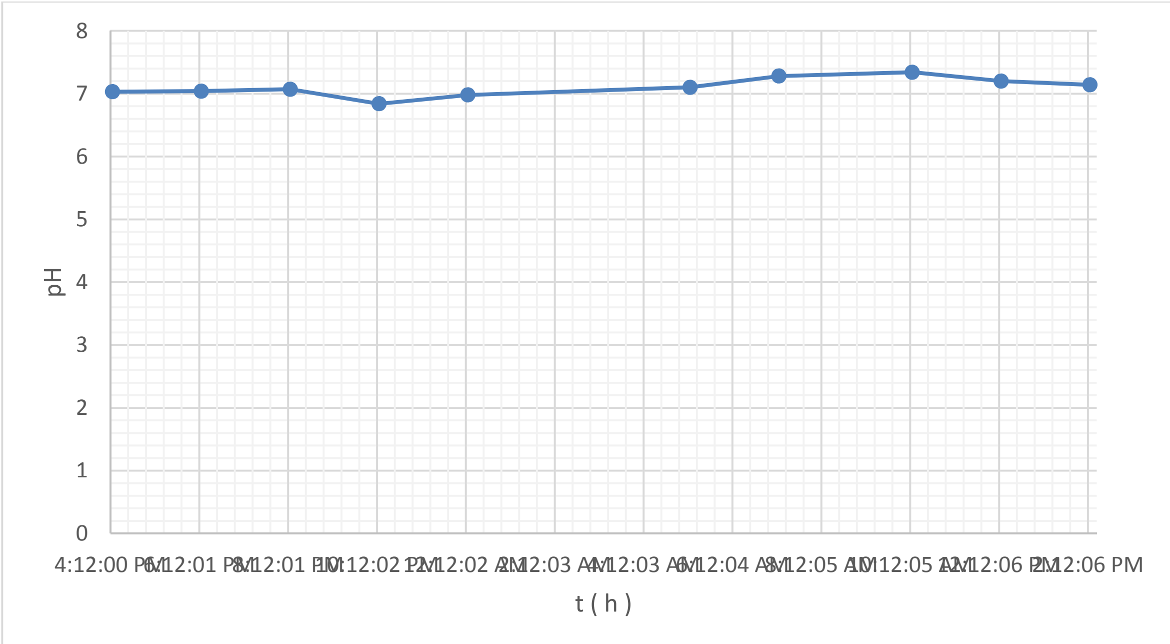

Figure 32: Results analyse campaign, pH, entrance of grit chamber

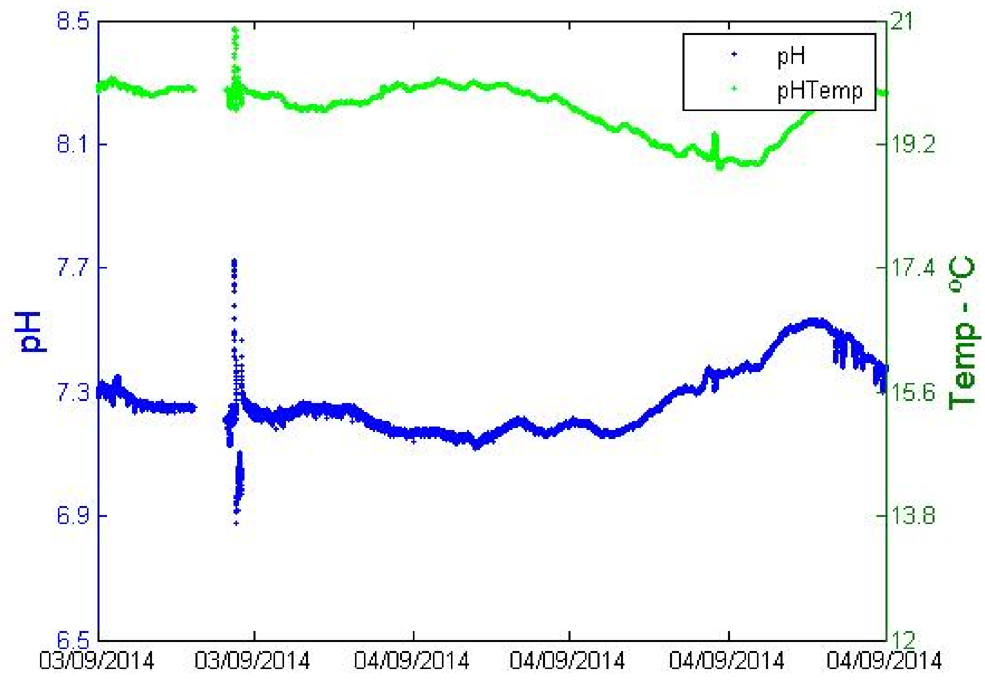

Figure 33: Data from monEAU station, pH, entrance of primary clarifier

For this sensor, the Sensolyt 700 IQ the value and the pattern are similar in laboratory analyze and in the data from the station. This sensor is ok.

We cannot compare the data from turbidity because we didn't analyse turbidity in laboratory.

8 CONCLUSION

This internship in Québec was a really good experience for many things. First I improved my knowledge about water quality sensors used in water treatment that will be useful in my career in water engineering. Second I improved my English level because the all the documents were in English and I spoke in English with my supervisor and with most of my friends which I met in Québec. And finally it was a really good personal experience, to see another way of life, to meet lot of people from all over the world. This experience really changed my mind.

9 REFERENCE

Beaupré M. (2010). Characterization of on-line sensors for water quality monitoring and process control. Master thesis, model*EAU*, Université Laval Quebec Canada.

Burket. Technical and commercial document, pH and ORP probe functioning. http://www.burkert.fr/products_data/datasheets/DS8203-standard-FR-FR.pdf

Daly, J (2010). ISA Norcal president. What is turbidity? http://www.isanorcal.org/download/tech2007_presentations/turbidity.pdf

Emersonprocess. Technical and commercial document, ORP probes functioning. http://www2.emersonprocess.com/siteadmincenter/PM%20Rosemount%20Analytical%20Documents/Liq_ADS_43-014.pdf

ISO (2003). Water quality – On-line sensors/analysing equipment for water-specifications and performances tests. ISO Standard 15839. Geneva, Switzerland.

Mauriel M. (2010). Evaluation of sensors and data procesing tools. Aquafit4use report.

metrohm. Technical and commercial document, electrode functioning. http://www.metrohm.fr/ph_metre/Images/Theorie%20electrode.pdf

Rieger, L and Vanrolleghem, P.A. (2008). monEAU: a platform for water quality monitoring networks, IWA Publishing 2008, Water Science & Technology.

s::can, User Manual, Spectrometer Probe V2 November 2011 release. http://www.ecs.umass.edu/eve/facilities/equipment/SCAN/Probemanual.pdf

YSI, a xylem brand: “IQ SensorNet Visoturb® 700 IQ Sensors”. https://www.ysi.com/accessoriesdetail.php?IQ-SensorNet-TetraCon-700-IQ-Sensors-166.

11 APPENDIX

11.1 Definitions of response time, delay time, rise and fall time

In this section the definitions (ISO15839:2003) are explained used to evaluate the temporal response to step changes as shown in Figure 34.

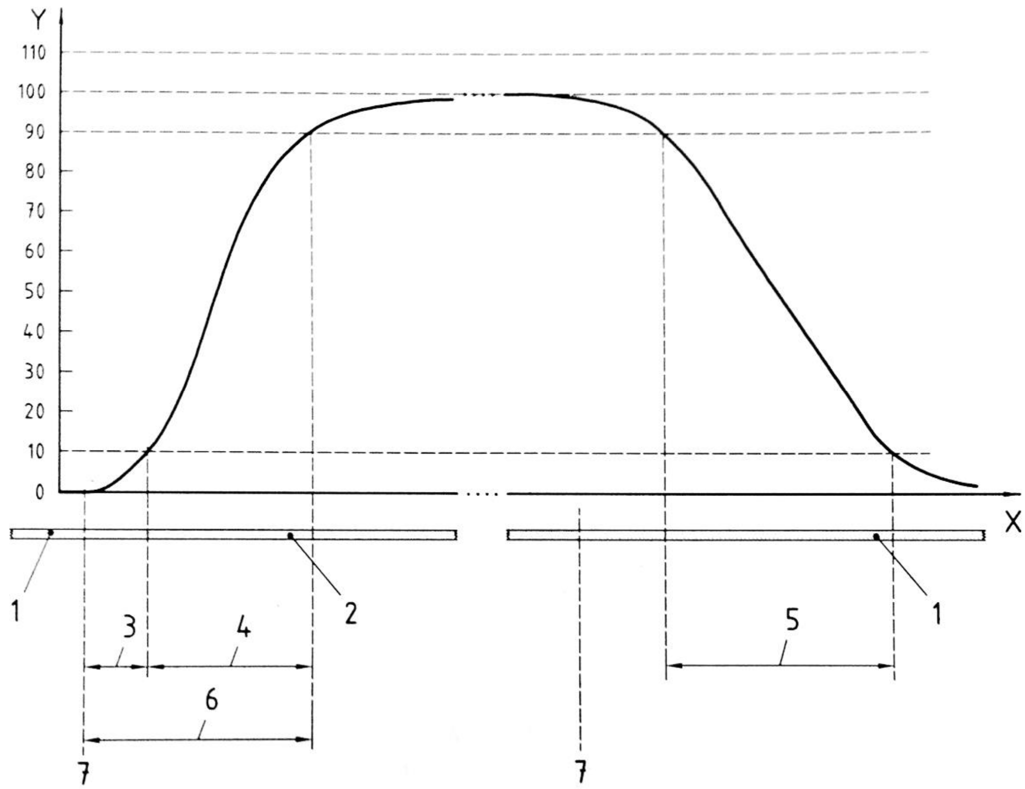

Key

X time
Y response (%age of value of abrupt change)

1 test solution (20 %)
2 test solution (80 %)
3 delay time
4 rise time
5 fall time
6 response time
7 change

Figure 34: Temporal response to a step change (ISO15839:2003)

11.1.1 Response time

Time interval between the instant when the on-line sensor/analysing equipment is subjected to an abrupt change in determinant value and the instant when the readings cross the limits of (and remain inside) a band defined by 90% and 110% of the difference between the initial and final value of the abrupt change (see Figure 34).

11.1.2 Delay time

Time interval between the instant when the on-line sensor/analysing equipment is subjected to an abrupt change in determinant value and the instant when the readings pass (and remain beyond) 10% of the difference between the initial and final value of the abrupt change (see Figure 34).

11.1.3 Rise time

Difference between the response time and the delay time when the abrupt change in determinand value is positive (see Figure 34).

11.1.4 Fall time

Difference between the response time and the delay time when the abrupt change in determinant value is negative (see Figure 34).

11.2 Definitions of Linearity, Coefficient of variation, limit of detection, limit of quantification, repeatability, lowest detectable change, bias, short-term drift and day-to-day repeatability

Some mathematical definitions which were used to evaluate different characteristics of the sensor are summarized in this section.

For a series of N measurements the mean $\overline{x}$ of the sample is calculated as:

$$\overline{x} = \frac{\sum_{i=1}^{N} x_i}{N}$$

(1)

The standard deviation is calculated as:

$$S_{xo} = \sqrt{\frac{1}{N}\sum_{i=1}^{N}\left(x_i - \overline{x}\right)^2}$$

(2)

where x_i the concentration of the ith standard sample and $\overline{x}$ the mean.

11.2.1 Linearity

Condition in which measurements made on calibration solutions having determinant values spanning the stated range of the on-line sensor/analysing equipment have a straight-line relationship (linear regression) with the calibration solution determinant values.

Based on the information at the Table 6 the linear regression model is calculated as:

$$y_{ij} = a + b \cdot x_i \quad (3)$$

where:

i is the determinand value level

j is the number of measurements for each determinand value level

x_i is the value of the determinant in the i^{th} calibration solution

y_{ij} is the j^{th} measurement of the determinant value x_i expressed in units of x

a is the intercept point of the regression line

b is the slope of the regression line

$a + b \cdot x_i$ represent the expectation of the measurement value of the i^{th} determinant value level

Table 6: Measurements required for linearity calculation

Reference sample (i)	Reference value (x_i)	Measurements (y_{ij})			
1	x_1	$y_{1,1}$	$y_{1,2}$	…	$y_{1,p}$
2	x_2	$y_{2,1}$	$y_{2,2}$	…	$y_{2,p}$
⋮	⋮	⋮	⋮	⋮	⋮
n	x_n	$y_{n,1}$	$y_{n,2}$	…	$y_{n,p}$

The parameters of the regression line are obtained as follows:

- Mean of p measurements of the i^{th} determinant value level

$$y_i = \frac{1}{p}\sum_{j=1}^{p} y_{ij}$$

- Mean of all determinant value levels

$$M_x = \frac{1}{n}\sum_{i=1}^{n} x_i$$

- Mean of all measurements

$$M_y = \frac{1}{n}\sum_{i=1}^{n} y_i$$

- Estimated slope b

$$b = \frac{\sum_{i=1}^{n}(x_i - M_x)\cdot(y_i - M_y)}{\sum_{i=1}^{n}(x_i - M_x)^2}$$

- Estimated intercept point a

  $a = M_y - b \cdot M_x$

- Correlation coefficient

$$R^2 = \frac{\left(\sum_{1}^{n}(x_i - M_x)\cdot(y_i - M_y)\right)^2}{\sum_{1}^{n}(x_i - M_x)^2 \sum_{1}^{n}(y_i - M_y)^2}$$

Results can be analyzed by mean the correlation coefficient R, which ideally should be equal to 1, and by using graphs (representation of the values measured against the reference values). An example is shown in Figure 35.

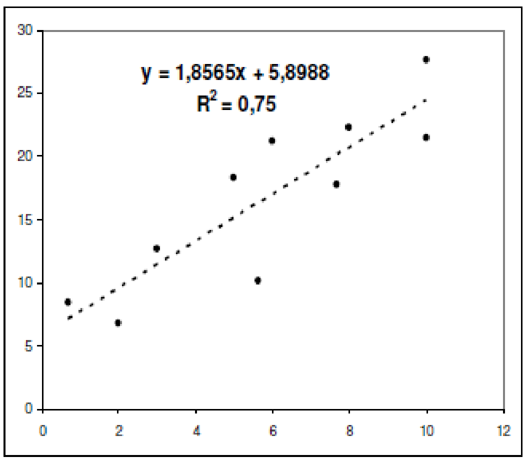

Figure 35.Example of linear regression (Mauriel M. (2010))

11.2.2 Coefficient of variation

Ratio between the standard deviation of the on-line sensor/analysing equipment and the mean of the working range of the equipment.

11.2.3 Limit of detection (LOD)

Lowest value, significantly greater than zero, of a determinant that can be detected. It is equal to three times the standard deviation (s_{xo}) of 6 measurements carried out at 5% of the measuring range.

$$LOD = 3 \cdot S_{xo(5\%)} \quad (4)$$

11.2.4 Limit of quantification (LOQ)

Lowest value of a determinant that can be determined with an acceptable level of accuracy and precision. It is equal to ten times the standard deviation (s_{xo}) of 6 measurements carried out at 5% of the measuring range.

$$LOQ = 10 \cdot S_{xo(5\%)} \quad (5)$$

11.2.5 Lowest detectable change (LDC)

Smallest significantly measurable difference between two measurements. It is equal to three times the standard deviation (s_{xo}) of 6 measurements carried out at 20% and 80% of the measuring range.

$$\begin{aligned} LDC_{20\%} &= 3 \cdot S_{xo(20\%)} \\ LDC_{80\%} &= 3 \cdot S_{xo(80\%)} \end{aligned} \quad (6)$$

11.2.6 Bias

Consistent deviation of the measured value from an accepted reference value. It is obtained by calculation of the difference between the average value of six measurements carried out at 20% and 80% of the measuring range and the value of reference measurement at each concentration respectively ($x_{20\%}, x_{80\%}$).

$$\begin{aligned} B_{20\%} &= \bar{x}_{20\%} - x_{20\%} \\ B_{80\%} &= \bar{x}_{80\%} - x_{80\%} \end{aligned} \quad (7)$$

11.2.7 Short-term drift

Slope of the regression line derived from a series of measurements carried out on the same calibration solution during laboratory testing, and expressed as a percentage of the measurement range over a 24 h period.

11.2.8 Long term drift

Slope of the regression line derived from a series of differences between reference and measurement values obtained during field testing, expressed as a percentage of the working range over a 24 h period.

11.2.9 Repeatability

Precision under repeatability conditions. It is equal the standard deviation (s_{xo}) of 6 measurements carried out at 20% and 80% of the measuring range.

$$\begin{aligned} R_{20\%} &= S_{xo(20\%)} \\ R_{80\%} &= S_{xo(80\%)} \end{aligned} \quad (8)$$

11.2.10 Day-to-day repeatability

Precision under day-to-day repeatability conditions. It is equal to ten times the standard deviation (s_{xo}) of 6 measurements carried out at 35% and 65% of the measuring range.

$$R_{35\%} = 10 \cdot S_{xo(35\%)}$$
$$R_{65\%} = 10 \cdot S_{xo(65\%)}$$
(9)

11.3 Memory effect

Temporary or permanent dependence of readings on one or several previous values of the determinant. The memory effect is typically observed as a saturation effect caused by the fact that a determinant value is well above the working range of the equipment. If the memory effect is permanent one, it will typically introduce a positive offset in the equipment.

11.4 Measurements and Calculations

11.4.1 VisoTurb 700 IQ n°13380866

Table 7: Measurements of the VisoTurb700IQ n°13380866

Percentage of the working range	Reference, xi	yi,1	yi,2	yi,3	yi,4	yi,5	yi,6
[%]	NTU	NTU	NTU	NTU	NTU	NTU	NTU
5	20	19.65679932	19.1495991	19.1704998	19.1648006	19.36000061	19.16640091
20	80	80.64769745	80.2720032	80.7424011	80.5673981	80.39649963	77.15869904
35	140	148.0279999	142.684006	140.362	144.082993	145.7910004	146.201004
50	200	199.3670044	201.949997	200.748001	202.367004	201.3079987	202.0140076
65	260	252.9519958	258.549011	261.751007	261.669006	261.1149902	262.928009
80	320	323.1300049	323.791992	323.863007	323.766998	324.4960022	323.5880127
95	380	384.0239868	383.101013	383.744995	383.770996	384.1289978	383.1390076

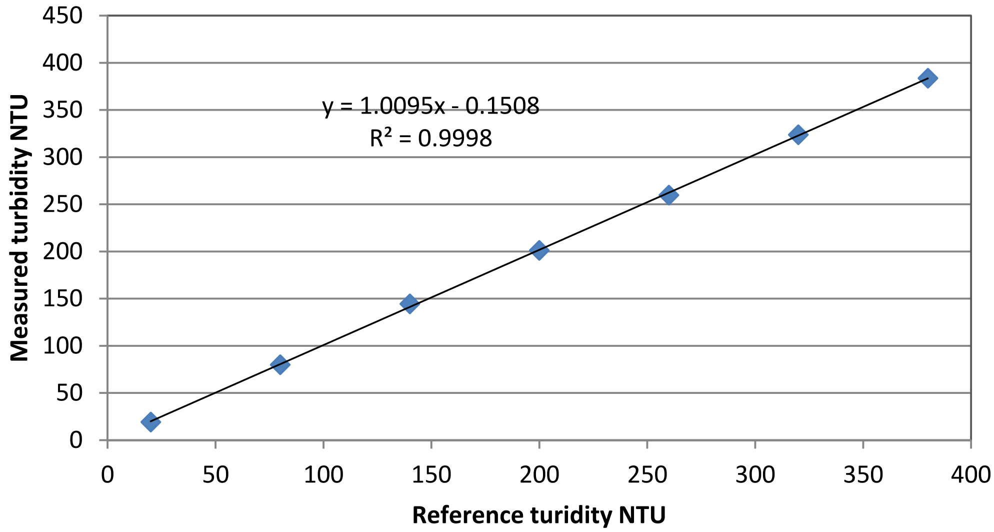

Figure 36: Linearity calculation of VisoTurb 700 IQ n°13380866

11.4.2 VisoTurb 700IQ n°13450270

Table 8: Measurements of the VisoTurb700IQ n°13450270

Percentage of the working range	Reference, xi	yi,1	yi,2	yi,3	yi,4	yi,5	yi,6
[%]	NTU	NTU	NTU	NTU	NTU	NTU	NTU
5	20	20.61359978	20.7574005	20.6152	20.6891003	20.6410999	21.00790024
20	80	89.74990082	85.2418976	84.782402	85.1516037	84.9974976	84.79959869
35	140	155.0930023	148.268997	146.242004	149.970993	149.910995	151.7019958
50	200	206.522995	206.800003	207.132004	207.311005	207.429001	207.7890015
65	260	257.2080078	263.546997	265.046997	266.289001	268.371002	267.4309998
80	320	325.9630127	326.579987	327.438995	327.786987	327.380005	327.178009
95	380	383.125	383.063995	375.076996	383.005005	383.274994	382.8890076

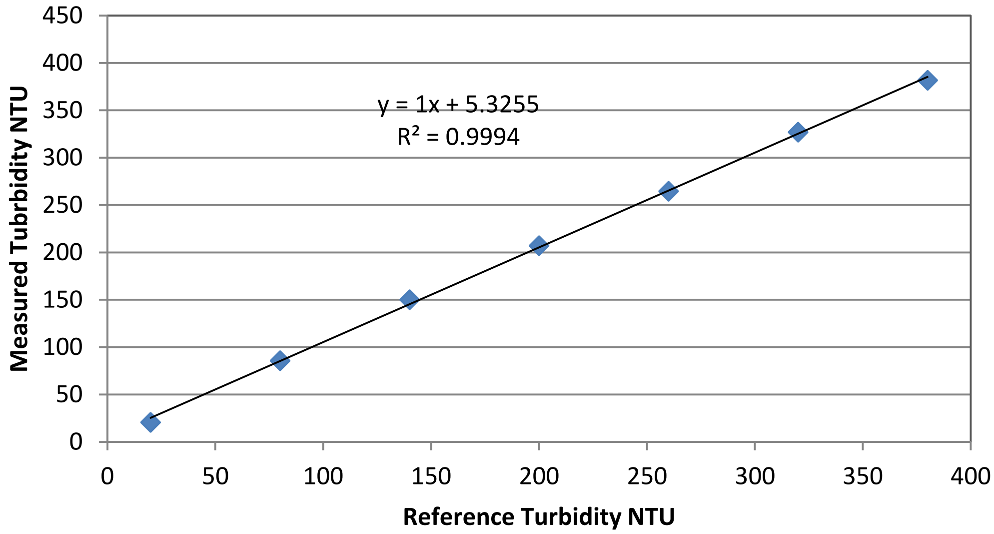

Figure 37: Linearity calculation of VisoTurb 700 IQ n°13450270

Table 9: Memory effect calculation VisoTurb 700 IQ n°13450270

X%	y1	y2	y3	y4	y5	y6	/X	Memory effect NTU
20	80.48	81.37	81.62	81.82	82.15	83.11	81.7583491	1.758349101

11.4.3 VisoTurb 700 IQ n°13450272

Table 10: Measurements of the VisoTurb700IQ n°13450272

Percentage of the working range	Reference, xi	yi,1	yi,2	yi,3	yi,4	yi,5	yi,6
[%]	NTU	NTU	NTU	NTU	NTU	NTU	NTU
5	20	22.315	20.776	23.760	21.401	22.788	18.703
20	80	83.933	84.001	84.033	83.834	83.906	84.112
35	140	154.827	147.775	145.436	154.203	147.993	148.828
50	200	208.678	208.874	208.685	208.691	208.562	208.616
65	260	256.885	263.018	269.018	272.539	269.769	266.800
80	320	325.426	325.745	325.859	332.566	326.396	326.133
95	380	382.785	382.545	383.219	382.612	382.925	379.806

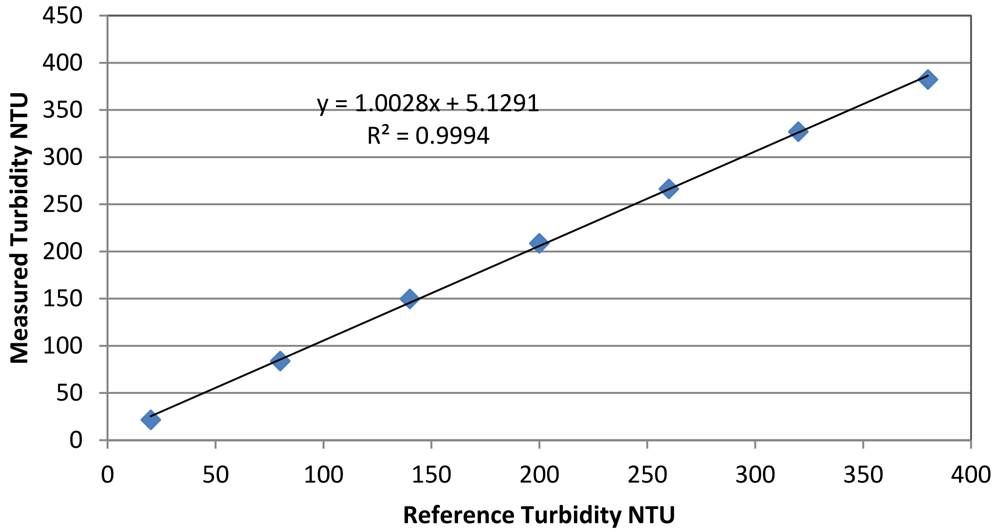

Figure 38: Linearity calculation of VisoTurb 700 IQ n°13450272

Table 11: Memory effect calculation VisoTurb 700 IQ n°13450272

X%	y1	y2	y3	y4	y5	y6	/X	Memory effect NTU
20	80.545	81.497	80.351	80.325	82.989	82.994	81.4499677	1.449967702

11.4.4 VisoTurb 700 IQ n° 13450271

Table 12: Measurements of the VisoTurb700IQ n°13450271

Percentage of the working range	Reference, xi	yi,1	yi,2	yi,3	yi,4	yi,5	yi,6
[%]	NTU	NTU	NTU	NTU	NTU	NTU	NTU
5	20	19.187	20.765	22.465	18.642	19.280	19.245
20	80	79.362	78.673	78.523	78.250	79.975	78.535
35	140	141.660	137.892	137.094	139.048	139.751	139.485
50	200	196.586	197.047	195.265	195.711	196.301	195.571
65	260	241.894	248.880	251.056	251.241	250.954	251.892
80	320	307.138	307.323	307.967	308.286	307.878	308.269
95	380	374.635	373.042	374.274	374.133	374.309	374.371

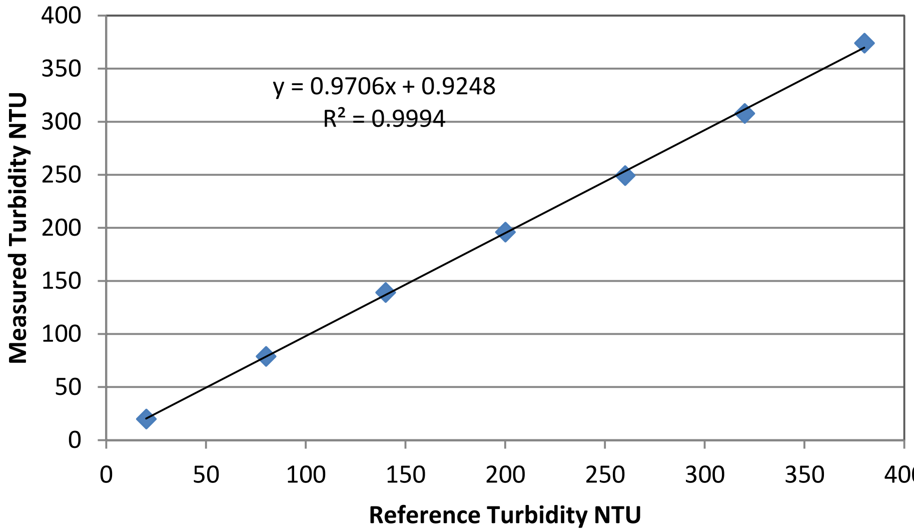

Figure 39: Linearity calculation of VisoTurb 700 IQ n°13450271

Table 13: Memory effect calculation VisoTurb 700 IQ n°13450271

X%	y1	y2	y3	y4	y5	y6	/X	Memory effect NTU
20	78.786	79.066	81.925	79.465	81.465	80.945	80.276	0.276

11.4.5 VisoTurb 13380867

Table 14: Measurements of the VisoTurb700IQ n°13380867

Percentage of the working range	Reference, xi	yi,1	yi,2	yi,3	yi,4	yi,5	yi,6
[%]	NTU	NTU	NTU	NTU	NTU	NTU	NTU
5	20	20.350	20.137	20.178	20.122	20.074	20.172
20	80	82.591	81.364	82.370	82.140	82.246	82.178
35	140	147.450	145.298	142.537	145.410	146.485	145.227
50	200	205.478	205.578	205.029	207.112	205.895	204.648
65	260	252.735	262.438	264.473	265.897	263.655	263.622
80	320	321.454	320.617	320.489	322.259	321.405	323.386
95	380	383.620	381.174	380.356	381.507	380.843	381.206

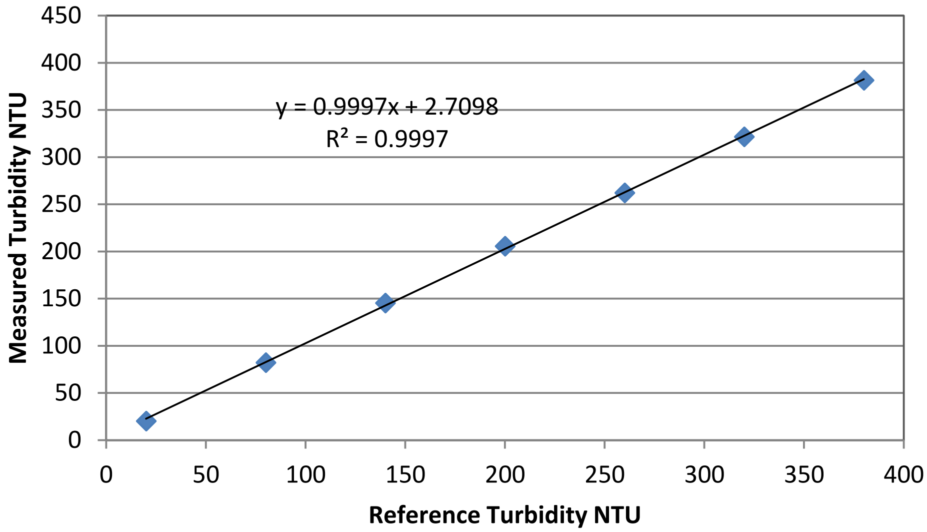

Figure 40: Linearity calculation of VisoTurb 700 IQ n°13380867

Table 15: Memory effect calculation VisoTurb 700 IQ n°13380867

X%	y1	y2	y3	y4	y5	y6	/X	Memory effect NTU
20	77.368	78.601	78.449	78.795	79.996	80.213	78.904	-1.096

11.4.6 VisoTurb 13380868

Table 16: Measurements of the VisoTurb700IQ n°13380868

Percentage of the working range	Reference, xi	yi,1	yi,2	yi,3	yi,4	yi,5	yi,6
[%]	NTU	NTU	NTU	NTU	NTU	NTU	NTU
5	20	20.779	21.062	20.779	22.402	21.033	21.145
20	80	92.411	86.942	86.122	83.375	83.459	83.603
35	140	149.203	150.030	145.541	150.651	147.961	148.480
50	200	211.273	211.469	210.503	211.804	211.804	212.601
65	260	261.901	269.379	270.354	271.674	270.986	270.501
80	320	322.734	324.073	324.160	323.704	325.012	325.841
95	380	389.496	388.672	389.170	389.689	388.968	388.678

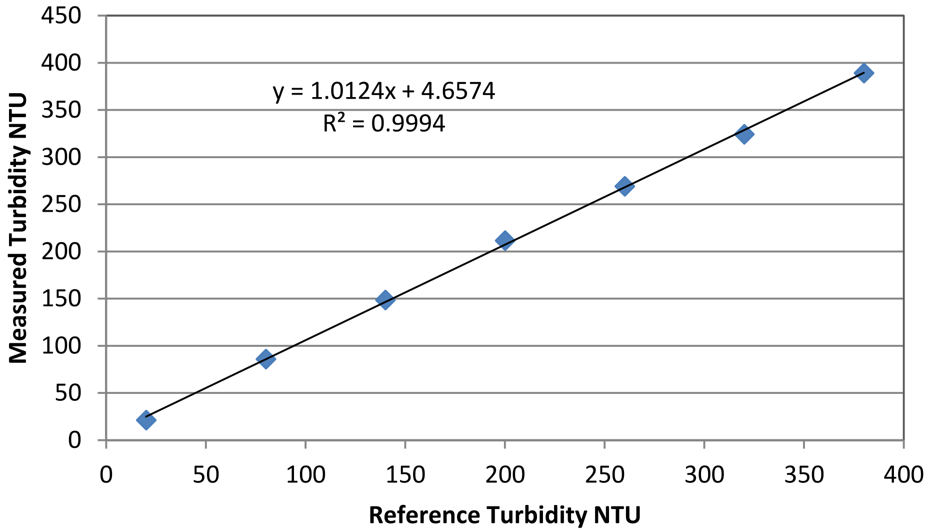

Figure 41: Linearity calculation of VisoTurb 700 IQ n°13380868

Table 17: Memory effect calculation VisoTurb 700 IQ n°13380868

X%	y1	y2	y3	y4	y5	y6	/X	Memory effect NTU
20	82.954	81.338	81.521	82.230	82.555	82.934	82.256	2.256